



# Dual-feedback mid-infrared cavity-enhanced absorption spectroscopy for H<sub>2</sub>CO detection using a radio-frequency electrically-modulated interband cascade laser

QIXIN HE,<sup>1,2</sup> CHUANTAO ZHENG,<sup>1,2,\*</sup> MINHAN LOU,<sup>2</sup> WEILIN YE,<sup>2,3</sup> YIDING WANG,<sup>1</sup> AND FRANK K. TITTEL<sup>2</sup>

<sup>1</sup>State Key Laboratory of Integrated Optoelectronics, College of Electronic Science and Engineering, Jilin University, 2699 Qianjin Street, Changchun 130012, China

<sup>2</sup>Department of Electrical and Computer Engineering, Rice University, 6100 Main Street, Houston, Texas 77005, USA

<sup>3</sup>College of Engineering, Shantou University, 243 Daxue Road, Shantou 515063, China

\*zhengchuantao@jlu.edu.cn

**Abstract:** A mid-infrared cavity-enhanced sensor system was demonstrated for the detection of formaldehyde (H<sub>2</sub>CO) using a continuous-wave (cw) interband cascade laser (ICL) centered at 3599 nm. A compact Fabry-Perot (F-P) cavity with a physical size of 38 × 52 × 76 mm<sup>3</sup> was developed consisting of two concave mirrors with a radius of curvature of 80 mm and a reflectivity of 99.8% at 3.6 μm. Different from the widely reported electro-optical (EO) external modulation based Pound-Drever-Hall (PDH) locking technique, a radio-frequency electrical internal modulation based PDH technique was used for locking the laser mode to the cavity mode. A dual-feedback control on the laser current and on the piezo transducer (PZT) displacement was utilized for further stabilizing mode locking. A 20 m effective optical path length was achieved with a cavity length of 2 cm and a finesse of 1572. The effectiveness and sensitivity of the sensor system were demonstrated by targeting an absorption line at 2778.5 cm<sup>-1</sup> for H<sub>2</sub>CO measurements. A linear relation between the cavity transmitted signal amplitude and the H<sub>2</sub>CO concentration was obtained within the range of 0–5 ppm. A 1σ detection limit of 25 parts-per-billion (ppb) was achieved with an averaging time of 1 s based on Allan-Werle variance analysis. The reported dual-feedback RF modulation based PDH technique led to a method for gas detection using a similar experimental setup and measurement scheme.

© 2018 Optical Society of America under the terms of the [OSA Open Access Publishing Agreement](#)

**OCIS codes:** (280.3420) Laser sensors; (300.6340) Spectroscopy, infrared; (140.5965) Semiconductor lasers, quantum cascade.

## References and links

1. W. Zhang, X. Cheng, X. Zhang, Y. Xu, S. Gao, H. Zhao, and L. Huo, "High selectivity to ppb-level HCHO sensor based on mesoporous tubular SnO<sub>2</sub> at low temperature," *Sens. Actuators B Chem.* **247**, 664–672 (2017).
2. D. Wang, M. Zhang, Z. Chen, H. Li, A. Chen, X. Wang, and J. Yang, "Enhanced formaldehyde sensing properties of hollow SnO<sub>2</sub> nanofibers by graphene oxide," *Sens. Actuators B Chem.* **250**, 533–542 (2017).
3. L. Dong, Y. Yu, C. Li, S. So, and F. K. Tittel, "Ppb-level formaldehyde detection using a CW room-temperature interband cascade laser and a miniature dense pattern multipass gas cell," *Opt. Express* **23**(15), 19821–19830 (2015).
4. H. I. Schiff, D. R. Hastie, G. I. Mackay, T. Iguchi, and B. A. Ridley, "Tunable diode laser systems for measuring trace gases in tropospheric air," *Environ. Sci. Technol.* **17**(8), 352A–364A (1983).
5. H. Dahnke, G. von Basum, K. Kleinermanns, P. Hering, and M. Mürzt, "Rapid formaldehyde monitoring in ambient air by means of mid-infrared cavity leak-out spectroscopy," *Appl. Phys. B* **75**(2–3), 311–316 (2002).
6. D. Rehle, D. Leleux, M. Erdelyi, F. Tittel, M. Fraser, and S. Friedfeld, "Ambient formaldehyde detection with a laser spectrometer based on difference-frequency generation in PPLN," *Appl. Phys. B* **72**(8), 947–952 (2001).
7. D. G. Lancaster, A. Fried, B. Wert, B. Henry, and F. K. Tittel, "Difference-frequency-based tunable absorption spectrometer for detection of atmospheric formaldehyde," *Appl. Opt.* **39**(24), 4436–4443 (2000).

8. P. Maddaloni, P. Malara, G. Gagliardi, and P. De Natale, "Two-tone frequency modulation spectroscopy for ambient-air trace gas detection using a portable difference-frequency source around 3  $\mu\text{m}$ ," *Appl. Phys. B* **85**(2–3), 219–222 (2006).
9. K. Tanaka, K. Miyamura, K. Akishima, K. Tonokura, and M. Konno, "Sensitive measurements of trace gas of formaldehyde using a mid-infrared laser spectrometer with a compact multi-pass cell," *Infrared Phys. Technol.* **79**, 1–5 (2016).
10. J. Li, U. Parchatka, and H. Fischer, "A formaldehyde trace gas sensor based on a thermoelectrically cooled CW-DFB quantum cascade laser," *Anal. Methods* **6**(15), 5483–5488 (2014).
11. S. Lundqvist, P. Kluczynski, R. Weih, M. von Edlinger, L. Nähle, M. Fischer, A. Bauer, S. Höfling, and J. Koeth, "Sensing of formaldehyde using a distributed feedback interband cascade laser emitting around 3493 nm," *Appl. Opt.* **51**(25), 6009–6013 (2012).
12. F. Capasso, "High-performance midinfrared quantum cascade lasers," *Opt. Eng.* **49**(11), 111102 (2010).
13. T. K. Boyson, P. J. Dagdigan, K. D. Pavey, N. J. FitzGerald, T. G. Spence, D. S. Moore, and C. C. Harb, "Real-time multiplexed digital cavity-enhanced spectroscopy," *Opt. Lett.* **40**(19), 4560–4562 (2015).
14. S. G. Baran, G. Hancock, R. Peverall, G. A. Ritchie, and N. J. van Leeuwen, "Optical feedback cavity enhanced absorption spectroscopy with diode lasers," *Analyst (Lond.)* **134**(2), 243–249 (2009).
15. P. S. Johnston and K. K. Lehmann, "Cavity enhanced absorption spectroscopy using a broadband prism cavity and a supercontinuum source," *Opt. Express* **16**(19), 15013–15023 (2008).
16. H. Yi, T. Wu, G. Wang, W. Zhao, E. Fertein, C. Coeur, X. Gao, W. Zhang, and W. Chen, "Sensing atmospheric reactive species using light emitting diode by incoherent broadband cavity enhanced absorption spectroscopy," *Opt. Express* **24**(10), A781–A790 (2016).
17. E. D. Black, "An introduction to Pound–Drever–Hall laser frequency stabilization," *Am. J. Phys.* **69**(1), 79–87 (2001).
18. R. Drever, J. L. Hall, F. Kowalski, J. Hough, G. Ford, A. Munley, and H. Ward, "Laser phase and frequency stabilization using an optical resonator," *Appl. Phys. B* **31**(2), 97–105 (1983).
19. C. E. Liekhus-Schmaltz, and J. D. D. Martin, "Understanding Pound-Drever-Hall locking using voltage controlled radio-frequency oscillators: An undergraduate experiment," *Am. J. Phys.* **80**(3), 232–239 (2012).
20. B. Burghardt, W. Jitschin, and G. Meisel, "Precise rf tuning for cw dye lasers," *Appl. Phys., A Mater. Sci. Process.* **20**(2), 141–146 (1979).
21. T. C. Briles, D. C. Yost, A. Cingöz, J. Ye, and T. R. Schibli, "Simple piezoelectric-actuated mirror with 180 kHz servo bandwidth," *Opt. Express* **18**(10), 9739–9746 (2010).
22. C. E. Liekhus-Schmaltz, R. Mantifel, M. Torabifard, I. B. Burgess, and J. D. D. Martin, "Injection-locked diode laser current modulation for pound-drever-hall frequency stabilization using transfer cavities," *JOSA. B* **29**(6), 1394–1398 (2012).
23. J. M. Langridge, T. Laurila, R. S. Watt, R. L. Jones, C. F. Kaminski, and J. Hult, "Cavity enhanced absorption spectroscopy of multiple trace gas species using a supercontinuum radiation source," *Opt. Express* **16**(14), 10178–10188 (2008).
24. S. Kassi, M. Chenevier, L. Gianfrani, A. Salhi, Y. Rouillard, A. Ouvrard, and D. Romanini, "Looking into the volcano with a MIR-IR DFB diode laser and Cavity Enhanced Absorption Spectroscopy," *Opt. Express* **14**(23), 11442–11452 (2006).
25. F. Wei, B. Lu, J. Wang, D. Xu, Z. Pan, D. Chen, H. Cai, and R. Qu, "Precision and broadband frequency swept laser source based on high-order modulation-sideband injection-locking," *Opt. Express* **23**(4), 4970–4980 (2015).
26. J. Li, Z. Du, and Y. An, "Frequency modulation characteristics for interband cascade lasers emitting at 3  $\mu\text{m}$ ," *Appl. Phys. B* **121**(1), 7–17 (2015).
27. A. Soibel, M. W. Wright, W. Farr, S. Keo, C. Hill, R. Q. Yang, and H. C. Liu, "High-speed operation of interband cascade lasers," *Electron. Lett.* **45**(5), 264–265 (2009).

## 1. Introduction

Formaldehyde ( $\text{H}_2\text{CO}$ ) is colorless, combustible, toxic, carcinogenic and commonly used in architectural ornament materials and many household products [1–2].  $\text{H}_2\text{CO}$  escaping from these materials may lead to poor indoor air quality that adversely affects human health. The permissible  $\text{H}_2\text{CO}$  exposure limit is 750 parts-per-billion (ppb) averaged for an eight-hour work day and a short-term exposure limit of 2 ppm averaged over 15 min according to the US Occupational Safety and Health Administration [3]. Therefore, the detection of  $\text{H}_2\text{CO}$  is important particularly in industrial and environmental monitoring. There are many methods that can detect  $\text{H}_2\text{CO}$ . Compared with spectrophotometry and electrochemical methods, optical methods based on infrared laser spectroscopy are more appropriate due to their high detection sensitivity and selectivity as well as non-contact measurement [4–11]. Interband cascade lasers (ICLs) cover a mid-infrared spectral range of 3–4  $\mu\text{m}$ , where a strong fundamental vibration-rotation spectrum of  $\text{H}_2\text{CO}$  molecular transitions can be found. Thus

ICLs with a smaller thermal dissipation and lower power consumption than quantum cascade lasers (QCLs) are more suitable for H<sub>2</sub>CO detection in the mid-infrared [12].

Fabry–Perot (F-P) cavity and multi-pass gas cell are two methods to enhance gas absorption. A multi-pass gas cell based H<sub>2</sub>CO sensor was reported by our group in 2015 [3]. With an integration time of < 1.5 s, a detection limit of ~3 ppb was achieved by using direct absorption spectroscopy (DAS) and a multi-pass cell with a 54.6 m optical path length. Compared to a multi-pass gas cell, a F-P cavity is simple in structure, easy to adjust, low in attenuation and small in volume [13–16]. The Pound–Drever–Hall (PDH) technique was used to frequency stabilize the excitation laser to the cavity, which was successfully demonstrated on laser frequency stabilization of various wavelengths [17–19]. In a PDH-locked cavity-enhanced sensor system, the laser is frequency modulated and a photodiode detector is used to measure the reflected light from the cavity. By mixing the diode signal with the modulating signal, an error signal is obtained to suppress the laser frequency fluctuations. Three methods to modulate the laser frequency: electro-optic modulation [20], acousto-optic modulation [21] and current-injection modulation [22] have been reported. Recently, the most commonly used method is electro-optic modulation.

In this work, a distributed feedback (DFB) ICL based Pound–Drever–Hall (PDH) locked cavity-enhanced H<sub>2</sub>CO sensor system was demonstrated. A compact, temperature controlled F-P cavity was designed and employed as a gas cell. The feasibility of locking the ICL to the F-P cavity by a radio-frequency (RF) electrical modulation based PDH technique was confirmed. This locking technique is different and novel from the reported electro-optical modulation based PDH locking technique [23]. Furthermore, a dual-feedback control on the laser current and on the piezo transducer (PZT) extension length was utilized to lock the laser mode to the cavity mode and to avoid a slow drift of the cavity length caused by environmental temperature changes and vibrations. Design, calibration, and long-term stability measurements of H<sub>2</sub>CO sensor system are presented. The reported RF electrical modulation based PDH technique and dual-feedback control technique have led to an effective technique for sensitive and selective gas detection using a similar experimental setup and measurement scheme.

## 2. Cavity-enhanced H<sub>2</sub>CO sensor system design

### 2.1. Sensor architecture

The design of the cavity-enhanced sensor system is depicted in Fig. 1. A continuous-wave (cw) DFB ICL (Nanoplus), centered at a wavelength of ~3.6  $\mu\text{m}$  was operated by a commercial laser controller (Vescent photonics, D2-105-500) for high-frequency current modulation with an input frequency over 1 GHz. The laser controller has an ultra-low current noise with a noise density < 100 pA/Hz<sup>1/2</sup> and a two-stage proportional–integral–derivative (PID) temperature control with a sub-mK temperature stability. A high-frequency sine-wave signal (120 MHz, 10 mV) was generated by a function signal generator (Tektronix, AFG3102) to modulate the laser frequency. An optical isolator (Thorlabs, IO-4-3400-WG) with an isolation of 25 dB at 3.6  $\mu\text{m}$  was used to prevent the reflected light from the cavity getting back into the ICL. Two lenses (concave lens M2 with a focal length of – 8 cm; convex lens M3 with a focal length of 10 cm) were used to match the waist of the beam (~0.8 mm) to the Fabry–Perot cavity and thereby eliminating the higher order modes as well as producing a clean error control signal.

The radiation emitted by the ICL was reflected by the first cavity mirror and then focused on a photodetector (VIGO, PVI-2TE-4) through a convex lens M5 with a focal length of 5 cm. This detector has a detectivity of  $6 \times 10^{11}$  cm·Hz<sup>1/2</sup>/W, a noise level of 0.95 nV·Hz<sup>1/2</sup> and a high cutoff frequency of 200 MHz. The output signal from the detector passed through a high-pass filter (HPF) and was subsequently mixed with the ICL modulation signal via a mixer. The lower cutoff frequency of the HPF is set to 10 MHz to bypass the 120 MHz

modulation signal and suppress the low-frequency noise. A low-pass filter (LPF1, upper cutoff frequency is 1.9 MHz) was used after the output of the mixer to obtain a low-frequency signal as an error signal. The output of the LPF1 was directed to a PID controller (PID1, Toptica, PID110), which can provide a control signal to adjust the ICL current, locking the ICL mode to the cavity mode. A second feedback loop was used to eliminate the low frequency drift of the cavity length, which consists of a low-pass filter (LPF2), a PID controller (PID2) and a PZT controller. A very low cutoff frequency of 1 Hz of LPF2 was set to achieve a slow error signal for cavity-length adjustment. The PID parameters should be selected for a rapid, accurate and stable mode locking procedure (PID1) and suppression of the cavity-length drift (PID2). At resonance, a transmission signal from the cavity was produced. The transmitted ICL beam was focused by a concave mirror M8 with a focal length of 5 cm and detected by the photodiode detector (VIGO, PVI-4TE-5), whose detectivity is  $6 \times 10^{10} \text{ cm} \cdot \text{Hz}^{1/2} / \text{W}$  and cut-off frequency is 100 KHz. The detector signal was delivered to a laptop via a DAQ card for data recording and post analysis.

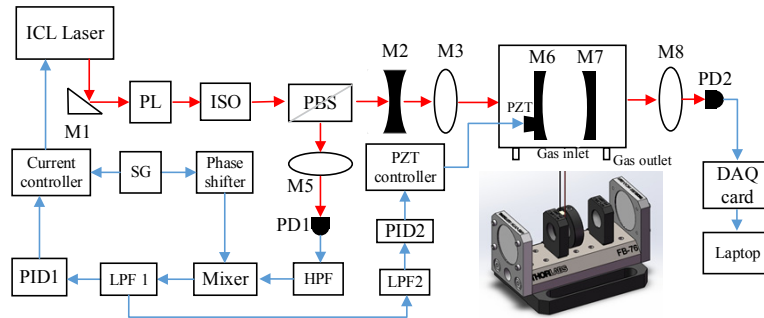


Fig. 1. Structure of the RF modulation based PDH-locked cavity-enhanced  $\text{H}_2\text{CO}$  sensor system with a dual-feedback control on the laser current and PZT displacement. Red lines are optical paths and blue lines are signal paths. ICL, interband cascade laser; PBS, polarizing beam splitter; PZT, piezoelectric transducer; DAQ, data acquisition; PD, photodiode detector; LPF, low-pass filter; HPF, high-pass filter. The inset shows the schematic of the designed cavity.

Table 1. Basic specifications of the designed cavity.  $c$  is the light speed in the cavity.

Cavity length	$L$	2 cm
Reflectivity	$R$	99.8%
Free spectral range	$FSR = c/(2L)$	7.5 GHz
Finesse	$F = \pi\sqrt{R}/(1-R)$	1572
Linewidth	$\Delta\nu = FSR/F$	4.77 MHz
Effective optical path length	$L_{\text{eff}} = 2L\sqrt{R}/(1-R)$	20 m

Cavity-enhanced absorption spectroscopy (CEAS) is based on the use of optical cavities in order to enhance light interaction with a gas species inside the cavity [24]. The schematic of the cavity is shown in the inset of Fig. 1. The cavity is composed of two concave mirrors (LohnStar Optics, USA) with a radius of curvature of 80 mm and a reflectivity of  $R = 99.8\%$  at  $3.6 \mu\text{m}$ . The mirrors were fixed to a single-axis fiber bench. The cavity was sealed with a plastic cover with a gas inlet and an outlet. One of the cavity mirrors was fixed to a  $3.6 \mu\text{m}$  displacement piezo chip (Thorlabs, PA4FKW) to make the cavity length adjustable. The basic properties of the cavity are illustrated in Table 1. Furthermore measures were taken in order to provide environmental stabilization of the cavity. An aluminum enclosure was used with two windows for access to the optical components inside. The inside of the enclosure was covered with a layer of fiber glass insulation to reduce acoustic vibrations. The cavity was

fixed to a pressurized air floating optical table via an aluminum base and a rubber mat was added under the cavity to reduce mechanical vibrations. A custom PID temperature controller with an accuracy of  $-0.01\sim0.01$  °C was used to minimize temperature fluctuations.

## 2.2 $\text{H}_2\text{CO}$ line selection and characterization of the ICL laser

$\text{H}_2\text{CO}$  has a fundamental vibrational band with its C-H symmetric ( $\nu_1$ ) stretching mode at  $2785\text{ cm}^{-1}$  [9–11]. A transmission spectra of 100 ppb  $\text{H}_2\text{CO}$  and standard air (with a mixture of 1.8%  $\text{H}_2\text{O}$ , 320 ppb  $\text{N}_2\text{O}$ , 1.8 ppm  $\text{CH}_4$ ) in the spectral region from  $2774$  to  $2784\text{ cm}^{-1}$  was simulated using the HITRAN 2012 database, as shown in Fig. 2(a) and Fig. 2(b), where the pressure was 700 Torr, the temperature was 296 K and the optical path-length was 20 m. An absorption line located at  $2778.5\text{ cm}^{-1}$  was selected due to its large absorption coefficient. The  $\text{H}_2\text{CO}$  absorbance is 0.0038 for a 20 m absorption path length and a 100 ppb  $\text{H}_2\text{CO}$  concentration. As can be seen from Fig. 2(a), the  $\text{H}_2\text{O}$  absorption line near  $2778.5\text{ cm}^{-1}$  interferes with  $\text{H}_2\text{CO}$  detection. In order to eliminate the interference of water vapor, a commercial drier (W.A. Hammond Drierite, CAS #7778-18-9) was used. Other gases present in air have minimal interference to  $\text{H}_2\text{CO}$  detection.

A high precision wavelength meter (Bristol Instruments, 671 Series) was employed to measure the output wavelength of the ICL. The wavelength tuning characteristics of the ICL dependence on temperature and current are shown in Fig. 2(c). The driving current was varied from 30 mA to 50 mA and the ICL's operating temperature was changed from  $30\text{ °C}$  to  $38\text{ °C}$ . The temperature and current tuning coefficients were  $0.7\text{ nm/°C}$  and  $0.19\text{ nm/mA}$ , respectively. When the laser temperature and current were set to  $33.7\text{ °C}$  and 45 mA, the ICL emission wavelength can target the  $2778.5\text{ cm}^{-1}$   $\text{H}_2\text{CO}$  absorption line.

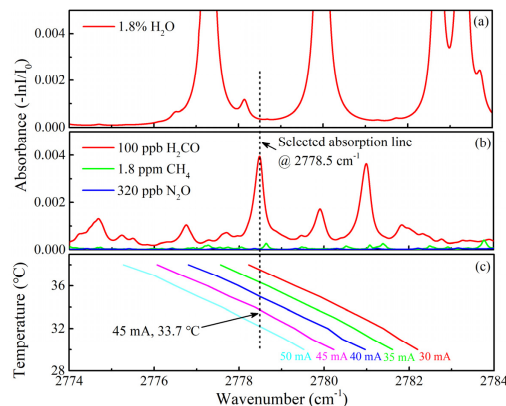


Fig. 2. (a)  $\text{H}_2\text{O}$  absorption line near  $2780\text{ cm}^{-1}$ . (b) Atmospheric  $\text{H}_2\text{CO}$  absorption line located near  $2780\text{ cm}^{-1}$  in comparison with  $\text{N}_2\text{O}$  and  $\text{CH}_4$ . (c) Tuning characteristics of the  $3.6\text{ }\mu\text{m}$  ICL.

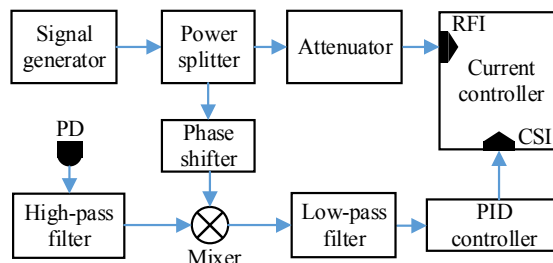


Fig. 3. The electronic feedback loop of the RF electrical modulation based PDH locking method. RFI, Radio frequency input; CSI, Current servo input; PD, photodiode; PID, proportional–integral–derivative.



### 2.3 RF electrical modulation based PDH locking technique

Generally, semiconductor lasers are able to operate at high frequencies (with bandwidths in the GHz range) with appropriate packaging, as was verified for ICLs at low temperatures with operation up to 3.2 GHz [25–27]. In this work, the ICL temperature was maintained at 33.7 °C. At a driving current of 45 mA, the output power was 3.2 mW and the emission wavelength was near 3.6  $\mu\text{m}$ . The schematic of the electronic feedback loop is shown in Fig. 3. A sinusoidal RF signal with a frequency of 120 MHz was generated by the function signal generator (Tektronix, AFG3102) and then was divided into two parts by means of a power splitter. One part was applied to the current driver after passing through an attenuator in order to modulate the laser frequency. The other part was directed to a phase shifter and then was mixed with the filtered, reflected signal generated by a photo detector. A low-pass filter was used following the mixer to acquire a low-frequency signal as an error signal. This error signal was then processed by a PID controller and fed back to the laser current driver laser frequency tuning.

The laser intensity and frequency were modulated simultaneously by the 120 MHz sinusoidal current with an amplitude of 0.08 mA. The amplitude of the sinusoidal current was small enough compared to the bias current to ensure a linear current-to-wavelength behavior. Because of the small injection current, the residual amplitude modulation (RAM) has a small impact on gas detection. Besides, when the ICL mode was locked to the cavity mode, the output of the PID controller is close to zero and causes small fluctuations to light intensity. The frequency variation is 128 MHz resulting from the sinusoidal modulation. To observe the cavity resonance, a ramp signal (15 V, 0.5 Hz) was applied to the PZT as shown in Fig. 4(a). The transmitted signal and the error signal were observed using an oscilloscope as shown in Fig. 4(b) and 4(c) separately. The ramp signal was used to trigger the sampling of the cavity transmitted signal and the error signal for PID1. The higher order modes in Fig. 4(b) have little interference to the error signal in Fig. 4(c). With feedback, the system was found to operate in the steep linear region corresponding to the center of the error signal.

An assessment of the finesse can be made according to the cavity resonance transmission signal shown in Fig. 4. The modulation sideband can be used as a frequency reference to calculate the linewidth of the cavity ( $\Delta\nu$ ). Based on the linewidth and the FSR, the finesse can be calculated by  $F = \text{FSR}/\Delta\nu$ . The calculated linewidth  $\Delta\nu$  is 6.77 MHz and the finesse is 1108.

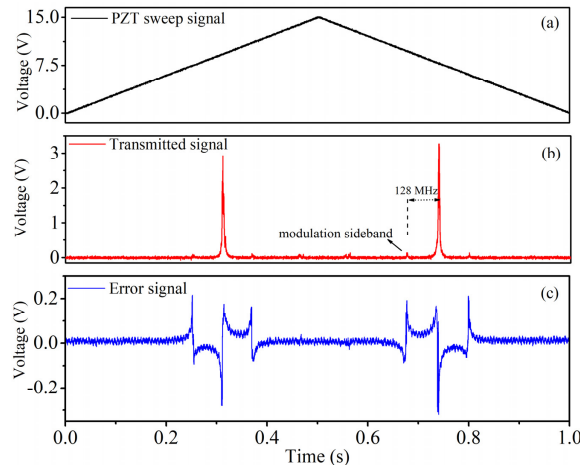


Fig. 4. Cavity resonance under critical coupling conditions. (a) PZT sweep signal. (b) Transmitted signal from the cavity. (c) Error signal generated by the mixer followed by a low-pass filter.

## 2.4 Dual-feedback control analysis

As shown in Fig. 1, in addition to the PDH feedback loop, another PID controlled negative feedback loop was used to eliminate the low frequency drift of the cavity length and optimize the long-term stability of the system. When the laser is locked to the cavity, the amplitude of the error signal is close to zero. Because of the change of environment in the long-term experiment, the cavity length will have a low frequency drift which will cause an offset of the error signal amplitude. A low-pass filter was used to extract the amplitude of the error signal and this extracted signal was directed to a PID controller and a cavity length control signal was generated. By selecting the appropriate PID parameters, the drift of the cavity length can be suppressed. During the experiment (Section 3.2), the laser wavelength was not tuned but was locked to the cavity mode by using the first PID loop. Since the cavity length was locked by the second PID loop, the laser wavelength was therefore locked to the H<sub>2</sub>CO absorption line.

## 3. Sensor performance

### 3.1. H<sub>2</sub>CO absorbance measurements

The following experiments were carried out in a 23 °C thermostatically controlled laboratory, and the pressure of the gas cell was controlled to be 700 Torr. Since the temperature change results in a larger wavelength variation than changing other parameters (e.g. current, cavity length), the ICL current was set to 45 mA and the operating temperature was varied from 33.55 °C to 33.7 °C in steps of 0.012 °C and the emission peak wavenumber was changed from 2778.15 cm<sup>-1</sup> to 2779.05 cm<sup>-1</sup>. The laser was locked to the cavity at each wavenumber by adjusting the PZT drive voltage and the average of the transmitted signal voltage in 1 minute was recorded by a custom data-recording and analyzing program based on the National Instruments LabVIEW platform with a data sampling rate of 50 Hz. An example of the absorption signal at a 10 ppm H<sub>2</sub>CO is shown in Fig. 5.

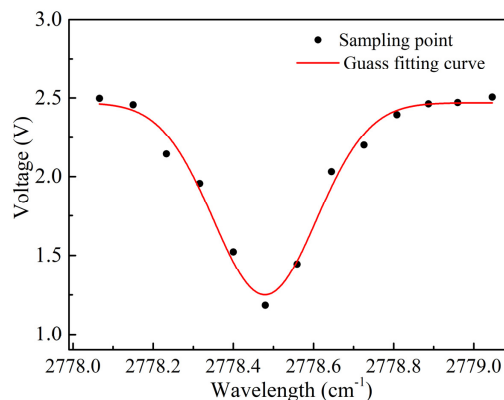


Fig. 5. An acquired absorption spectrum of 10 ppm H<sub>2</sub>CO by tuning the laser temperature from 33.55 °C to 33.7 °C in steps of 0.012 °C

### 3.2. Calibration experiment and stability

In this experiment, the laser temperature was set to 33.63 °C and the bias current was set to 45 mA. By using the dual-feedback RF modulation based PDH locking technique, the laser wavelength was continuously locked to the cavity resonant wavelength, i.e. the center wavelength of the H<sub>2</sub>CO absorption line. The transmitted power through the cavity was ~0.5 mW at a driving current of 45 mA under a pure nitrogen (N<sub>2</sub>) atmosphere. The transmitted signal from the cavity was acquired at a sampling frequency of 50 Hz. After data averaging, one spectral point was obtained per one second.

Different  $\text{H}_2\text{CO}$  samples balanced with pure  $\text{N}_2$  (0 ppm, 1 ppm, 2 ppm, 3 ppm, 4 ppm, 5 ppm) were generated by means of a commercial gas dilution system (EnviroNics, Model 4040) for sensor calibration. The linear response of the sensor system was investigated by measuring the cavity transmitted signals at different mixing ratios. The amplitude of the transmission signal was recorded and the relationship between the absorption signal amplitude and the  $\text{H}_2\text{CO}$  concentration is shown in Fig. 6(a). The measurement for each concentration level lasted for 5 minutes. As shown in Fig. 6(b), the acquired fitting equation between  $\text{H}_2\text{CO}$  concentration ( $C$ ) and the transmission signal amplitude ( $V$ ) is

$$V = 2.5 - 0.136C \quad (1)$$

where  $C$  is in ppm and  $V$  is in Volts.

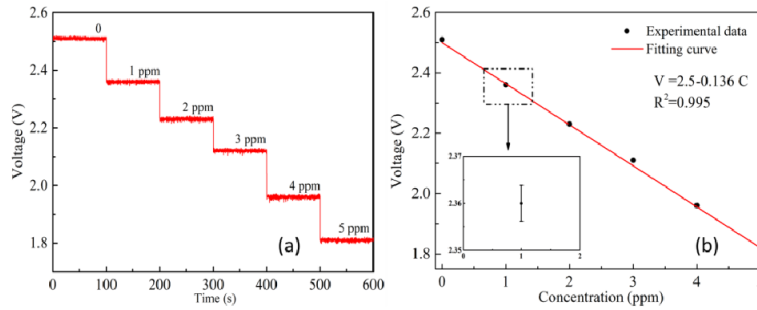


Fig. 6. (a) Cavity transmitted signal at different  $\text{H}_2\text{CO}$  concentration levels. (b) The fitting curve of the relationship between the averaged absorption signal amplitude and  $\text{H}_2\text{CO}$  concentration within the range 0–5 ppm. The inset shows the error bar of the 1 ppm  $\text{H}_2\text{CO}$  averaged amplitude.

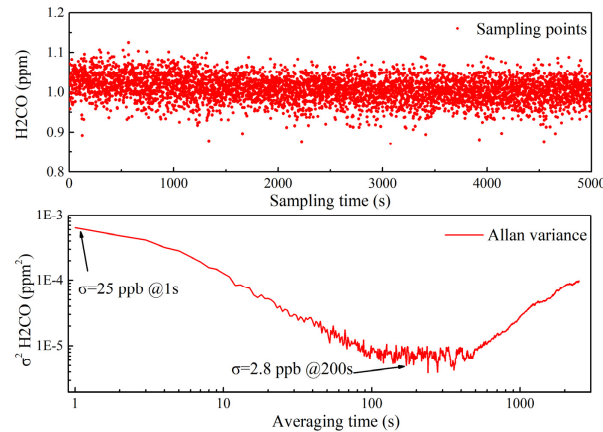


Fig. 7. The Allan variance plot of the sensor system (lower figure) based on the long-term concentration measurement results (upper figure) for the 1 ppm  $\text{H}_2\text{CO}$  sample.

An Allan-Werle variance analysis was performed to evaluate the long-term stability and precision of the  $\text{H}_2\text{CO}$  sensor system. The concentration of a  $\text{H}_2\text{CO}$  sample with a concentration level of 1 ppm was measured over a period of 100 minutes with a sampling period of 1 s. As shown in Fig. 7, a limit of detection of 25 ppb is obtained based on an Allan variance analysis for an averaging time of 1 s, which corresponds to an absorbance of 0.001, which is valid in a dry gas, free from water. When the averaging time increases to 200 s, the limit of detection (LoD) is 2.8 ppb. The noise that restricts the detection to an absorbance of 0.001 is due to the electrical noise coming from the laser driver, detector and DAQ card.



#### 4. Conclusions

By using dual-feedback RF modulation based PDH mode locking technique, a mid-infrared cavity-enhanced  $\text{H}_2\text{CO}$  sensor system was experimentally demonstrated by targeting an absorption line at  $2778.5\text{ cm}^{-1}$  for interference-free  $\text{H}_2\text{CO}$  measurement. A mid-infrared F-P cavity with a physical length of 2 cm and a finesse of 1572 was developed, leading to an absorption path length of 20 m. The performance of the sensor system, characterized by Allan-Werle variance analysis, was assessed and yielded a  $1\sigma$  LoD of 25 ppb with a 1 s averaging time. The LoD can be improved to 2.8 ppb with an averaging time of 200 s. The reported innovative dual-feedback and RF modulation based PDH technique can be applied to laser based chemical sensing of other target analytes using a similar experimental setup and measurement scheme. The signal-to-noise ratio of the system can be further improved by increasing the cavity length or using cavity mirrors with higher reflectivity, which will lead to higher sensor sensitivity and a lower LoD.

#### Funding

National Science Foundation (NSF) ERC MIRTHE Award; Robert Welch Foundation (No. R4925U); National Natural Science Foundation of China (NSFC) (Nos. 61775079, 61627823, 61307124); National Key R & D Program of China (Nos. 2016YFD0700101, 2016YFC0303902, 2017YFB0402800); Key Science and Technology “R & D” Program of Jilin Province, China (No. 20180201046GX); Science and Technology Planning Project of Guangdong Province, China (No. 2017A020216011); Industrial Innovation Program of Jilin Province, China (No. 2017C027).